Microbes and Infection xxx (xxxx) xxx

Contents lists available at ScienceDirect

Microbes and Infection

journal homepage: www.elsevier.com/locate/micinf

Single-cell transcriptome analysis of the early immune response in the lymph nodes of *Borrelia burgdorferi*-infected mice

Varpu Rinne [a,*], Kirsi Gröndahl-Yli-Hannuksela [a], Ruth Fair-Mäkelä [a,b], Marko Salmi [a,b,c], Pia Rantakari [a,d], Tapio Lönnberg [b,d], Jukka Alinikula [a], Annukka Pietikäinen [a,e], Jukka Hytönen [a,e]

[a] Institute of Biomedicine, Faculty of Medicine, University of Turku, Turku, Finland
[b] InFLAMES Research Flagship, University of Turku, Turku, Finland
[c] MediCity, Faculty of Medicine, University of Turku, Turku, Finland
[d] Turku Bioscience Centre, University of Turku and Åbo Akademi University, Turku, Finland
[e] TYKS Laboratories, Clinical Microbiology, Turku University Hospital, Turku, Finland

ARTICLE INFO

Keywords:
Single-cell RNA sequencing
Borrelia burgdorferi
Extrafollicular immune response
Lymphocyte
Murine model

ABSTRACT

Lyme borreliosis is a disease caused by *Borrelia burgdorferi* sensu lato bacteria. *Borrelia burgdorferi* is known to induce prolonged extrafollicular immune responses and abnormal germinal centre formation. The infection fails to generate a neutralizing type of immunity, eventually establishing a persistent infection. Here, we performed single-cell RNA sequencing to characterize the immune landscape of lymph node lymphocytes during the early *Borrelia burgdorferi* infection in a murine model.

Our results indicate key features of an extrafollicular immune response four days after *Borrelia burgdorferi* infection, including notable B cell proliferation, immunoglobulin class switching to IgG3 and IgG2b isotypes, plasmablast differentiation, and the presence of extrafollicular B cells identified through immunohistochemistry. Additionally, we found infection-derived upregulation of suppressor of cytokine signalling genes *Socs1* and *Socs3,* along with downregulation of genes associated with MHC II antigen presentation in B cells.

Our results support the central role of B cells in the immune response of a *Borrelia burgdorferi* infection, and provide cues of mechanisms behind the determination between extrafollicular and germinal centre responses during *Borrelia burgdorferi* infection.

1. Introduction

Lyme borreliosis, the most common vector-borne disease in Europe and the United States, is caused by *Borrelia burgdorferi* sensu lato bacteria (later: *B. burgdorferi*) [1,2]. A characteristic immune response to *B. burgdorferi* in its natural hosts serves to reduce and control the spirochete numbers and minimize the manifestations of the infection. However, the bacteria establish a persistent infection, enabling the re-acquisition of the spirochetes by ticks and their subsequent transmission to new hosts. Therefore, it seems likely that the co-evolution of *B. burgdorferi* and its reservoir host species has resulted in a state that maintains the enzootic cycle while helping the host avoid overt disease manifestations [3,4]. On the other hand, some host species develop a symptomatic inflammatory response, which is seen also in humans. Indeed, without antibiotic treatment, Lyme borreliosis can persist in humans for years. Whether this is due to a weak initial immune response or ineffective clearance of bacteria is not properly understood [5].

Early *B. burgdorferi* dissemination activates both innate and adaptive immune responses, resulting in macrophage and dendritic cell-mediated phagocytosis as well as eventually antibody-induced killing of the bacterial cells [3]. Immune response to *B. burgdorferi* is characterized by a lack of robust T-dependent B cell responses and impaired germinal centre formation [5]. In contrast, *B. burgdorferi* induces a prolonged extrafollicular response by poorly understood mechanisms [6]. It has been suggested that extrafollicular immune response is driven by strong antigen recognition [7]. Indeed, in *B. burgdorferi* infection, intact spirochetes are widely present in lymph nodes already in the early phase of the infection [8,9]. The extrafollicular response to *B. burgdorferi* is characterized by strong plasmablast (PB) responses in lymph nodes, and especially by an IgM, IgG3, and IgG2b dominant antibody production [4,

* Corresponding author. University of Turku, Institute of Biomedicine, Medisiina D7, Kiinamyllynkatu 10, 20500, Turku, Finland.
E-mail address: varrin@utu.fi (V. Rinne).

https://doi.org/10.1016/j.micinf.2024.105424
Received 22 November 2023; Received in revised form 30 August 2024; Accepted 13 September 2024
Available online 19 September 2024

9]. However, these extrafollicularly derived antibodies do not generate a long-term neutralizing type of immunity [10,11].

Here, we have focused on early-stage infection and have analysed single-cell RNA sequencing (scRNA-seq) profiles of draining lymph node lymphocytes from *B. burgdorferi*-infected mice. We provide evidence for plausible reduction of T cell – B cell interaction and bias for an extrafollicular response. The results give insight into the mechanisms behind the mainly extrafollicular *B. burgdorferi*-specific B cell response.

2. Materials and methods

2.1. Mouse infection, cell isolation, library preparation, and sequencing

Borrelia burgdorferi sensu stricto strain N40 was cultured in Barbour-Stoenner-Kelly II (BSK II) medium at +33 °C to a logarithmic phase of growth. Bacteria were washed twice with phosphate-buffered saline (PBS) and counted in a Neubauer cell counting chamber. Bacterial cells were concentrated to 50×10^6 bacteria/ml in PBS. Four female mice (C3H/HeN, aged 4 weeks) were infected by administering 20 μl of the bacterial suspension (10^6 bacteria/injection) subcutaneously into the hind-leg footpad (Microfine Demi 0.3 ml syringes with a 30-G needle, BD #324826). As a vehicle control, PBS (20 μl) was injected similarly into the other four mice. After four days, mice were sacrificed, and popliteal lymph nodes (draining lymph nodes for the hind leg) were harvested. Lymph nodes from infected mice were pooled into one sample and lymph nodes from control mice were pooled into another sample for lymphocyte isolation. In addition, iliac lymph nodes (further along the chain of draining lymph nodes for the hind leg) were collected and analysed separately with *ospA*-based qPCR to confirm infection. PCR was performed as previously described [12,13].

Single-cell suspension of lymphocytes was produced by mechanically homogenising the pooled popliteal lymph nodes with a custom-made metal cell strainer to detach cells from the stroma. Cells were washed twice with PBS with 2 % fetal calf serum (FCS) buffer and filtered through 77 μm silk. Cells were re-filtered through a 40 μm filter and suspended in RPMI medium with 2 % FCS buffer.

Extracted lymphocytes were processed with the Chromium platform (10X Genomics) for library preparation, and the barcoded scRNA-seq libraries were constructed using 10XGenomics Chromium Next GEM Single Cell 3′, Reagent Kit v3.1. Briefly, reverse transcription was performed to specific single-cell gel beads in the emulsion to produce full-length 10X barcoded cDNA from polyadenylated mRNA. The cDNA was amplified with PCR, followed by enzymatic fragmentation, end repair and A-tailing, adaptor ligation, and sample index PCR. Qualities of cDNA were ensured with Agilent Bioanalyzer 2100, and index PCR was made using Chromium i7 Multiplex Kit. Prepared libraries were sequenced using the Illumina Novaseq6000 Sequencing System (RRID: SCR_016387). Library preparation and sequencing were done in the Finnish Functional Genomics Center at Turku Bioscience.

2.2. Bioinformatic analysis

Raw data processing, including demultiplexing, read alignment, and quality control, was performed using the 10X Genomics Cell Ranger package version 3.1.0. Mouse genome, mm10 (GENCODE vM23/Ensembl 98) was used as a reference.

Bioinformatic analysis was performed with R (version 4.3.0 2023-04-21) and RStudio (version 203.03.0). For data analysis, SEURAT – R tool kit for bioinformatic analysis (version 4.0) was used [14].

The control group and *B. burgdorferi*-infected group were processed separately. Low-quality or dying cells, which exhibit extensive mitochondrial gene expression, or low-quality cells with very few genes or none, were identified. Cells with less than 10 % of mitochondrial RNA counts and more than 600 but less than 4000 genes were selected for the analysis.

Datasets from the infection and control groups were normalized and the results were log-transformed. A subset of features that exhibit high cell-to-cell variation were calculated to highlight biological signals. These features that were repeatedly variable across datasets were selected for the integration features. The data were integrated with identified anchors. The integrated data were scaled to ensure that each gene contributes equally to the downstream analysis.

Principal component analysis (PCA) was performed to scale the data to reduce the number of input variables and eventually to make the data easier to visualize. The true dimensionality of the dataset was determined with the JackStraw procedure. Shortly, a subset of the data was rearranged (1 % by default), and PCA was rerun, which constructs a "null distribution" of feature scores and repeats. Fifty dimensions were chosen for the JackStraw procedure. In addition, Elbow plot and dimensionality heatmaps were used to evaluate the lowest PC with biologically relevant information, and PC40 was chosen as a cut-off. Data clustering was constructed as they were iteratively grouped to optimize the standard modularity function. The resolution was set to 0.7 and PC 1:40.

Cell cluster identification was performed with the minimum percentage argument set to 0.4 and the threshold for log2 fold change set to 0.5. Differentially expressed genes between the infection group and the control group were calculated using a Wilcoxon rank sum test. Gene ontology analysis (GO) was made using the Metascape web tool [15].

2.3. Re-clustering of T helper cell and B cell subpopulations

The $CD4^+$ T helper and B cell clusters were selected and separately re-clustered with the previously mentioned protocol. Data re-clustering was constructed with the resolution 0.3 and PC 1:20 for B cells and the resolution 0.4 and PC 1:20 for $CD4^+$ T cells. For the cluster identification of $CD4^+$ T cells, the threshold for log2 fold change was set to 0.3, due to the higher similarity of the dataset. Trajectory analysis and ordering cells to pseudotime were performed with Monocle3 [16].

2.4. Immunofluorescence analysis

For the immunofluorescence analysis, two mice were injected with *B. burgdorferi* as above, and two additional mice were injected with Ovalbumin (Invivogen, vac-pova, conc. = 0.1 μg/μl) and Complete Freud's Adjuvant (CFA) (Sigma, 20 % of the volume fraction) to induce germinal centre reactions. As a vehicle control, PBS (20 μl) was injected similarly into two mice. Optimal cutting temperature medium blocks were prepared from the draining lymph nodes of mice four days after injection. Frozen sections were cut and stained to visualize all cells using DAPI (Invitrogen, conc. = 1 μg/ml), B cells using Alexa Fluor® 488-conjugated monoclonal antibody against B220 (BioLegend, cat. #103225, clone = RA3-6B2, conc. = 10 μg/ml), germinal centres and activated B cells using Alexa Fluor® 647-conjugated monoclonal antibody against GL7 (Biolegend, cat. #144606, clone = GL7, conc. = 10 μg/ml), endothelial cells using Alexa Fluor® 647-conjugated monoclonal antibody against CD31 (Biolegend, cat. #102416, clone = 390, conc. = 10 μg/ml), and lymphatic vessel endothelial cell using polyclonal antibody against Lyve1 (ReliaTech, cat. #103-PA50, conc. = 10 μg/ml) with Alexa Fluor™ 546-conjugated secondary antibody (Invitrogen, cat. #A11035, conc. = 5 μg/ml) with 5 % normal mouse serum. The stained sections were imaged using a Pannoramic MIDI scanner (3DHISTECH). Images were acquired and processed using SlideViewer (version 2.8, 3DHISTECH). To enhance fluorescence visualization of the images of germinal centre staining, the black-and-white intensity levels were adjusted as follows: for the FITC channel, 12–120; for the Cy5 channel, 15–150; and the DAPI channel, 25–255. During the processing of images from medullary sinus staining, the black-and-white intensity levels were set to 8–80 for the FITC channel, 5–50 for the Cy5 channel, and 8–80 for the TRITC channel.

2.5. Statistics

The Chi-Square test was used to analyse the significance of cell number differences between the infection and the control group. The Wilcoxon rank-sum test was used to identify the differentially expressed genes and compare the differences in the expression of genes of interest between the infection and the control group with R software. The significance of differentially expressed genes was evaluated by adjusted p-value, based on Bonferroni correction.

2.6. Data availability

All raw and processed scRNA-seq data is deposited in the GEO database and are publicly available as of the date of publication [17]. The accession number is GSE248267.

3. Results

3.1. Immune cell landscape

ScRNA-seq analysis was conducted four days post-infection in a *B. burgdorferi*-infected mouse model, in order to investigate the mechanisms of acute immune response (Fig. 1A). Infection was confirmed with *ospA* detecting PCR (data not shown). Altogether 8840 and 10112 cells were identified in the infection and the control group, respectively.

Clustering of the cells resulted in 20 initial clusters, each representing a different gene expression profile. Based on marker genes, we categorized the cells into ten major cell lineages including $CD4^+$ T cells (*Cd3e, Cd4*), $CD8^+$ T cells (*Cd3e, Cd8a*), T regulatory (Treg) cells (*Cd4, Foxp3, Cd25*), T follicular helper (T_{Fh}) cells (*Cd3e, Cd4, Icos),* natural killer (NK) cells (*Ccl5, Cd25, Prf1, Ncr1, Il18rap*), B cells (*Cd19, Ighd, Cd38*) PB (*Jchain, Sdc1, Prdm1*), dendritic cells (DC; *Ccl5, Tnfrsf9, Cd40*), plasmacytoid dendritic cells (pDC; *Cd38, Cd11, Siglech, Cd209a*) and macrophages (*Lyz2*)(Fig. 1B–D).

B-cells were significantly more frequent in the infection group,

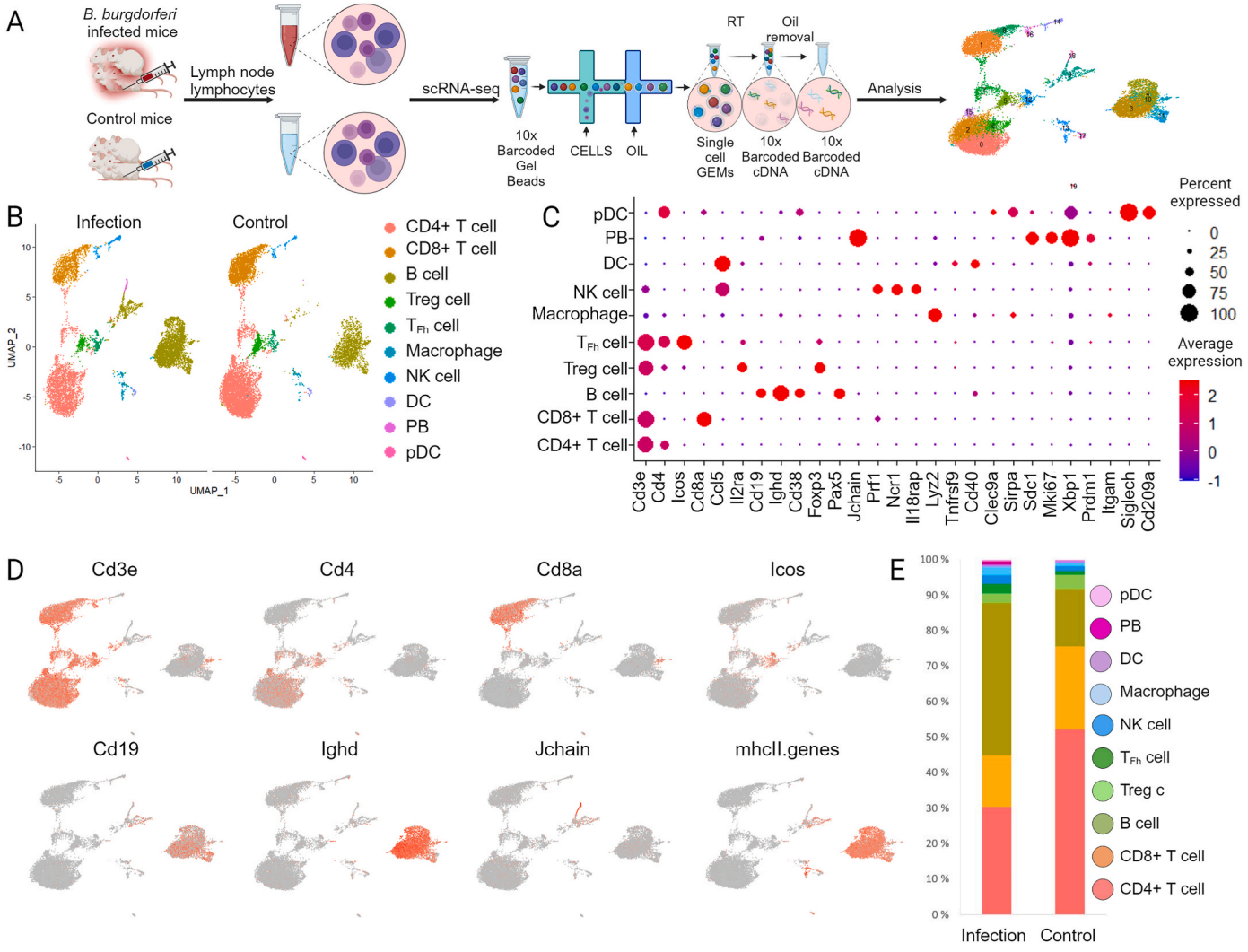

Fig. 1. Study workflow and the characterization of the immune cell clusters based on the scRNA-seq data.
(A) Experimental outline showing the lymphocyte collection and isolation after four days of infection. Library preparation and sequencing were performed with 10X Genomics® Chromium Single Cell Gene Expression method. (B) UMAP projection of major immune cell clusters from lymph nodes, showing the infection and the control groups respectively. Major cell clusters are shown in different colours. (C) The dot plot representing gene expression profiles of specific marker genes of each major cell lineage. (D) The feature plot showing the expression of selected marker genes across cell clusters. (E) The comparison of relative frequencies of cells of the major lineages in the infection and the control groups. (Abbreviations as follows: Treg: T regulatory, T_{Fh}: T follicular helper, NK: natural killer, DC: dendritic cell, PB: plasmablast, pDC: plasmacytoid dendritic cell).

constituting 43.9 % (3872 from the total 8840 cells) of the cells, compared to only 16.1 % (1633/10112) in the control group (p-value <0.00001) (Fig. 1E). T-cells, particularly CD4$^+$ T-cells, comprised a smaller proportion of the cells in the infection group as compared to the control group (30.4 % (2925/8840) vs. 52.2 % (5399/10112), p-value <0.00001).

To investigate the extrafollicular response and the previously suggested insufficient T – B cell interaction [5,6], we focused on B cell and CD4$^+$ T cell lineages in the subsequent analyses. Re-clustering of these lineages revealed some misclassified cells (Supplementary Figs. 1 and 2), which were excluded from further analysis.

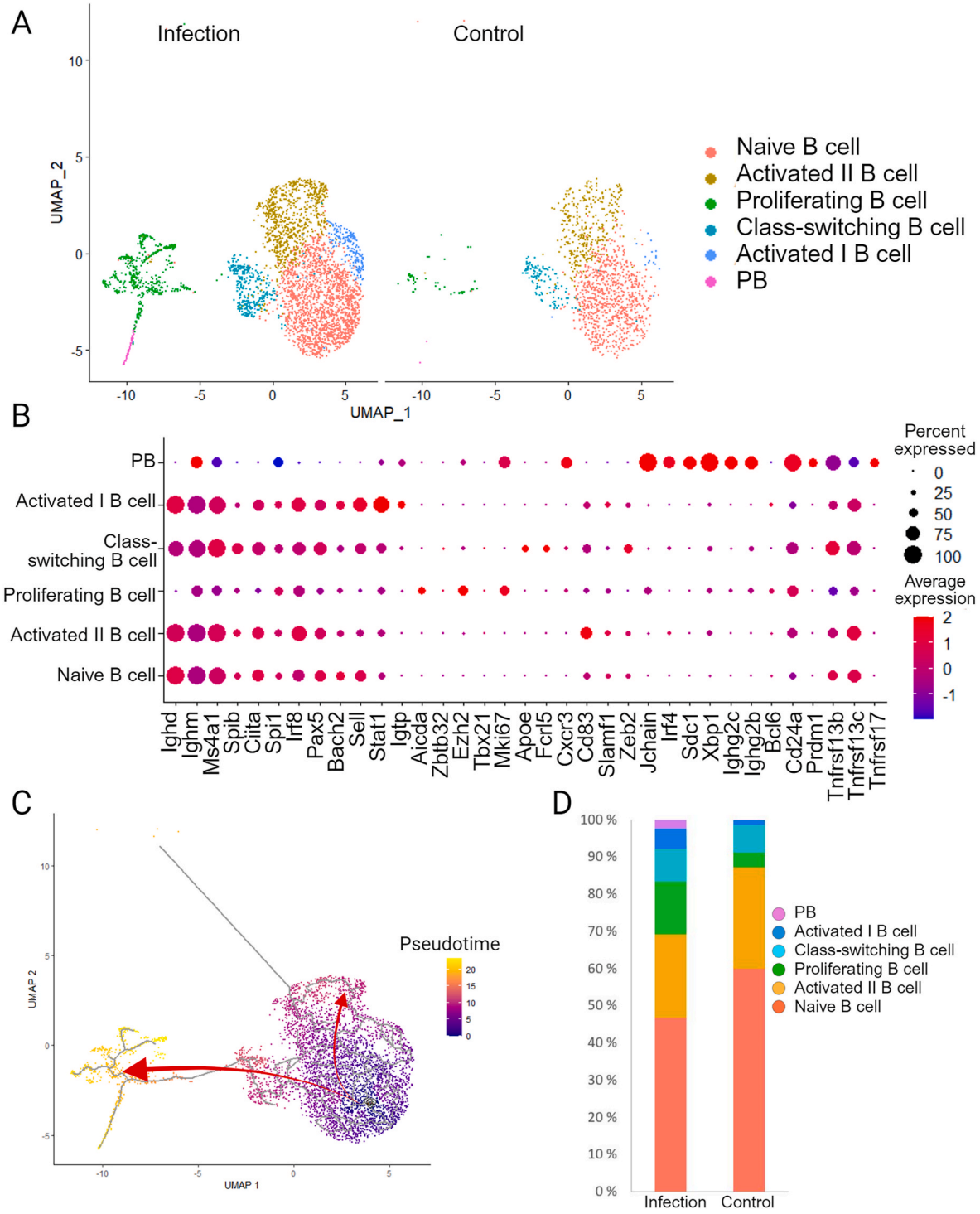

Fig. 2. B cell classification and differentially expressed genes between the infection and the control group.
(A) UMAP projection of identified B cell clusters, showing the infection and control groups, respectively. Cell clusters are shown in different colours. (B) Dot plot representing the gene expression profile of select marker genes of B cell subtypes. (C) Pseudotime analysis of the B cells suggesting a possible differentiation pathway of extrafollicular immune response (arrow pointing to the left from naive B cells towards the class switching B cells, proliferating B cells and the PB), and of cells that are primed for T cell-dependent response (arrow pointing to up/right from naive B cells towards cluster of activated II B cells). (D) The comparison of relative frequencies of B cell subtypes in the infection and the control groups.

3.2. B cell subsets

In the analysis of B cells, six different clusters with 3606 cells in the infection group and 1387 cells in the control group were included. (Fig. 2A). These six populations of B cells were identified based on their core markers and changes in the expression levels (↑ indicating upregulation and ↓ indicating downregulation in relation to other clusters) (Supplementary Table 1); naive B cells (*Ighd, Ighm, Ms4a1*), class-switching B cells (*Ighg2b*), proliferating B cells (*Cd19, Mki67*) and PB (*Jchain, Sdc1*) (Fig. 2A–B). We identified two clusters of B cells, which both displayed an activated phenotype, and labelled them as activated I B cells (*Ighd* ↓, *Ighm* ↑, *Stat1* ↑) and activated II B cells (*Ighd* ↓, *Cd83* ↑). TACI (*Tnfrsf13b*), a cytokine receptor associated with B cell survival during extrafollicular response, was upregulated in the class switching B cells. The cluster of activated I B cells expressed several interferon-induced genes and, thus, appears to be interferon-activated (Supplementary Table 1). Expression of *Cd83* in the cluster of activated II B cells indicates that the cells are prepared for T cell help, and the gene expression profile suggests that cells are primed for antigen presentation (Fig. 2B) (Supplementary Table 1). The cluster 'proliferating B cells' had a more prominent expression of genes related to cell cycle regulation, nucleotide synthesis, and replication. However, the cluster lacked evidence of secretory machinery expansion or expression of plasma cell transcription factor genes. Nonetheless, the detectable but low expression level of the joining chain of multimeric IgA and IgM (*Jchain)* suggests that these proliferating B cells have initiated the differentiation towards PB and the low expression of *Spi1* and *Irf8* suggests they do not participate in follicular response [18].

Pseudotime analysis suggests that proliferating B cells and PB represent distinct states compared to other B cell clusters (Fig. 2C). The cluster of activated I B cells was most similar to naive B cells representing similar differentiation stages in pseudotime. Overall, the trajectory analysis and pseudotime plot of the B cell subset suggest two distinct activation pathways, one for the rapid extrafollicular plasma cell differentiation and the other priming for a T cell-dependent response.

The clusters of activated I B cells, proliferating B cells, and PB were significantly enriched in the infection group (p-value <0.00001), whereas the cluster of activated II B cells formed a significantly smaller fraction of the cells (p-value 0.0002) (Fig. 2D). Thus, *B. burgdorferi* infection appears to induce B cell proliferation and PB differentiation via extrafollicular immune response at this time point.

3.2.1. Extrafollicular immune response

To further investigate the extrafollicular immune response, we compared the B cell activation and lymph node organization in response to *B. burgdorferi* versus a strong germinal centre-inducing stimulus (ovalbumin + CFA) and vehicle PBS control (Supplementary Fig. 3A) using immunofluorescence imaging. Four days after the footpad injection of *B. burgdorferi*, the draining lymph node exhibited a distinct B cell (B220+) staining pattern outside the follicular structures, possibly in the medullary cords. The follicles appeared disorganized, possibly due to strong accumulation of B cells [19]. There was some GL7 expression in the follicular area, which may indicate that B cells are activated and possibly prepared for the germinal centre response. As expected concerning the early time point, ovalbumin + CFA stimulus at the same time point did not exhibit germinal centre structures (GL7 negative), and the follicular appearance was preserved. Consistent with localization to medullary cords, where the chemokine CXCL12 is abundant [20], the induced PBs expressed *Cxcr4,* a receptor for CXCL12 (Supplementary Fig. 3B). These results support our conclusion that at day four post-*B. burgdorferi* footpad injection, the draining lymph node shows evidence of extrafollicular B cell activation.

To characterize the underlying gene expression programme of the extrafollicular response, we identified 252 differentially expressed genes in the B cell population between the infection and the control groups. The most substantial finding was the significant upregulation of genes associated with plasma cell differentiation (*Jchain*) and immunoglobulin class switching (*Ighg2b, Ighg3*) in the infection group (Fig. 3A–B) (see Supplementary Table 2 for significances). Furthermore, we observed that placenta specific 8 (*Plac8*), which is implicated in defence response against bacteria [21,22], and interferon gamma-induced proteasome 20S Subunit Beta 9 (*Psmb9*), important for MHC I antigen presentation [23], were both upregulated in the infection group.

We selected specific differentiation markers from the core markers of B cell clusters and analysed the infection and the control group separately. As expected, the expression of naive B cell marker *Ighd* and the B-lineage specification marker *Pax5*, both expressed at/until the mature stage of the B cell differentiation, were largely similar in infection and control groups (Fig. 3C). This indicates that not all B cells respond to *B. burgdorferi* antigens. However, the increase in infection-induced B cells with the expression of the *Ighg2b*, *Mki67*, and *Jchain* confirms immunoglobulin class switching, cell proliferation, and initiation of plasma cell differentiation. The particularly low expression of *Bcl6*, whose expression is required for initiation and maintenance of germinal centre reaction [24], strongly suggests that these populations are not derived from germinal centres (Fig. 2B, Supplementary Fig. 4A). In addition, comparison of differentiation and isotype switching markers show the notable upregulation of extrafollicular immunoglobulin class switching genes in the infection group (*Ighg2b, Ighg2c, Ighg3*) (Fig. 3D).

In conclusion, we observed a strong infection-derived immune response in B cells without evidence of germinal centres by both scRNA-seq and immunofluorescence staining. Therefore, the results support our hypothesis that B cells respond to *B. burgdorferi* primarily via extrafollicular immune response.

3.2.2. SOCS3 and downregulation of MHC II-related genes

To understand how *B. burgdorferi* might promote the extrafollicular response, we focused on the hypothesized regulation of antigen presentation by B cells. Interestingly, our analysis of differentially expressed genes between the infection and the control groups revealed significant infection-derived upregulation of suppressor of cytokine signalling genes *Socs1* and *Socs3* in B cells (Fig. 3A).

We subjected 40 of the most upregulated genes (log2 fold change >0.44) from the B cell subset in the infection group to Gene Ontology (GO) analysis (Fig. 3E–Supplementary Table 3). The analysis revealed significant enrichment of genes associated with Type II Interferon signalling and innate immune response. Interestingly, the observed gene expression pattern paralleled the one reported with *Salmonella* infection (Fig. 3E) [25]. The enrichment summary of the GO analysis revealed negative regulation of tyrosine phosphorylation of STAT protein, negative regulation of receptor signalling pathway via JAK-STAT, and negative regulation of receptor signalling pathway via STAT. Upregulation of three genes, *Socs3*, *Socs1,* and *Irf1,* was involved in the negative regulation of these biological processes, suggesting active inhibition of JAK-STAT pathways of cytokine signalling by Socs proteins.

Alongside the upregulation of *Socs1* and *Socs3*, we saw a significant downregulation of genes that are functionally related to antigen presentation via MHC II (*Ciita, Cd74, Cd40, H2-Aa, H2-DMb2, Ctss*) (Fig. 3A). To investigate whether the downregulation of the MHC II-related genes in the infection group was attributed to PB differentiation, we excluded the proliferating cells and PB from the analysis. Consequently, only subsets with naive and activated B cells (class switching B cells, clusters of activated I and II B cells) were included in this analysis. Despite this refinement, MHC II-related genes continued to exhibit downregulation in the infection group, particularly within the naive B cell cluster (Fig. 4A).

The inhibition of the JAK-STAT signalling pathway is known to reduce MHC II-related gene expression [26]. In agreement with the Socs-mediated downregulation of JAK-STAT pathway activation, violin plots visualize a consistent change in the expression of several genes involved in MHC II-mediated antigen presentation (*Ciita, Cd74, Cd40, H2-Aa, H2-DMb2, Ctss)* between the infection and the control groups,

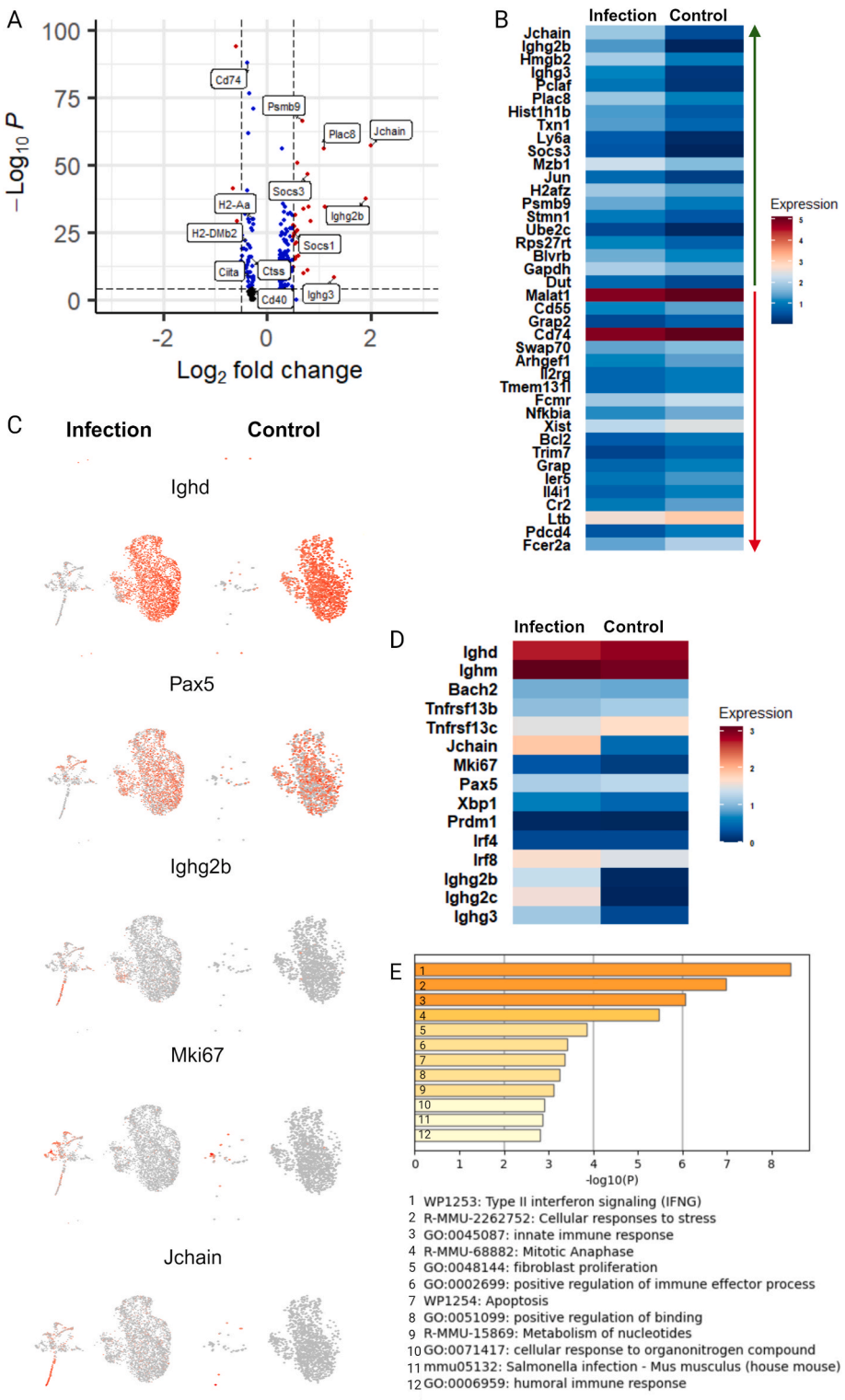

Fig. 3. Extrafollicular immune response

(A) A volcano plot showing differentially expressed B cell genes in the infection group compared to the control group. The X-axis represents the fold change between the groups on a log2 scale. The Y-axis shows negative log10 of the p-values. Selected genes are labelled. 252 variables were plotted, black dots represent no significance variation, blue dots represents significance in either Log2FC or p-value, and red dots represent significance for both, Log2FC and p-value. (B) Heatmap of 20 up- and downregulated genes of the infection group compared to the control group. The heatmap includes plasma blast/cell differentiation and immunoglobulin class switching markers that were upregulated in the infection group. (C) Feature plots showing the expression of selected specific differentiation markers from the core markers of B cell clusters, the infection and the control group visualized separately. The feature plots highlight the immunoglobulin class switching, cell proliferation and plasma cell differentiation due to *B. burgdorferi* infection. (D) Heatmap of differentiation and isotype switching markers. (E) GO analysis of 40 most upregulated genes of the infection group compared to the control group in all B cells. The graphic is showing the signalling pathways enriched in B cells in *B. burgdorferi* infection.

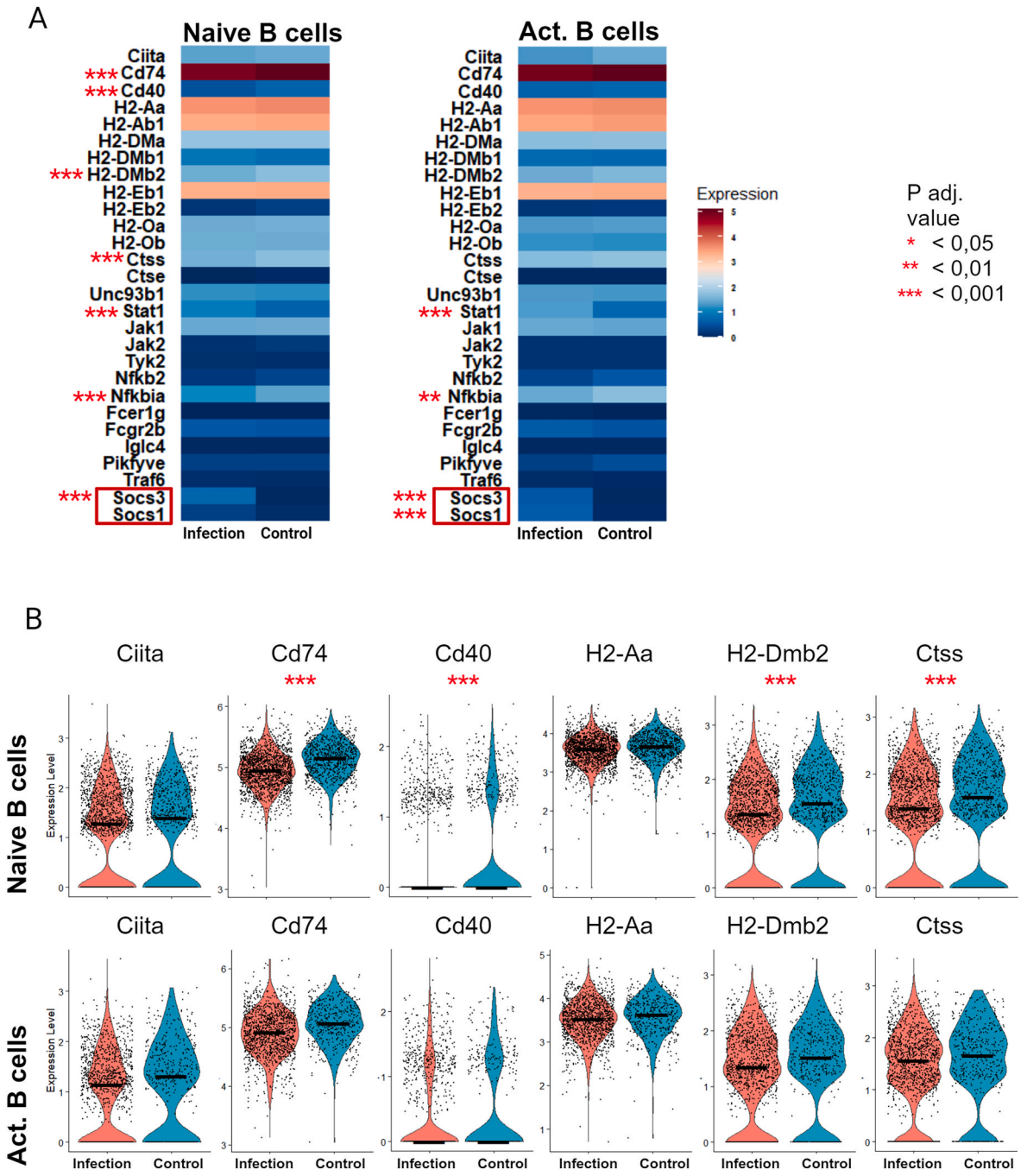

Fig. 4. Expression of MHC II -related genes

(A) Heatmap representation of expression levels of MHC II and JAK-STAT pathway-related genes in naive and activated B cells (including class switching B cells, clusters of activated I and II B cells) of the infection and the control group. Significant differences between the groups are pointed out with red asterisks. (B) Violin plot representation of some MHC II related genes in naive B cell and activated B cell populations. Plots with median value visualize the differences in the expression of genes between the infection and the control group. Statistically significant differences between the groups are shown with red asterisks. * = adjusted P value < 0.05; ** = adjusted P value < 0.01; *** = adjusted P value < 0.001.

even though all the differences are not statistically significant (Fig. 4B).

Overall, our dataset has no discernible indication of infection-driven upregulation of MHC II-related genes. These results imply that down-regulation of the MHC class II transactivator *Ciita* might occur via increased expression of *Socs3* after *B. burgdorferi* infection, which subsequently leads to inhibition of antigen presentation by B cells to T cells.

3.3. $CD4^+$ T cell subsets

In total, five initial clusters, 2960 in the infection group and 5536 cells in the control group were selected for further analysis of $CD4^+$ T cells. We identified five cell lineages, each representing distinct differentiation stages based on key marker genes; naive $CD4^+$ T cells (*Ccr7, Sell, Klf2, Mif* ↓), Treg cells (*Foxp3*), activated $CD4^+$ T cells (*Cd69, Mif*), T_{Fh} cells (*Icos, Cxcr5, Pdcd1*) and T helper 1 (T_{H1}) cells (*Stat1, Ms4a4b*) (Fig. 5 A-B, Supplementary Table 4). Activated $CD4^+$ T cells expressed *Stat6*, suggesting their differentiation into T helper 2 cells. T_{Fh} cells and T_{H1} cells were significantly enriched in the infection group (p-value <0.00001) (Fig. 5C). The infection group was composed only of 69.8 % (1875 of 2960) of naive $CD4^+$ T cells compared to 87.3 % (4456 of 5536)

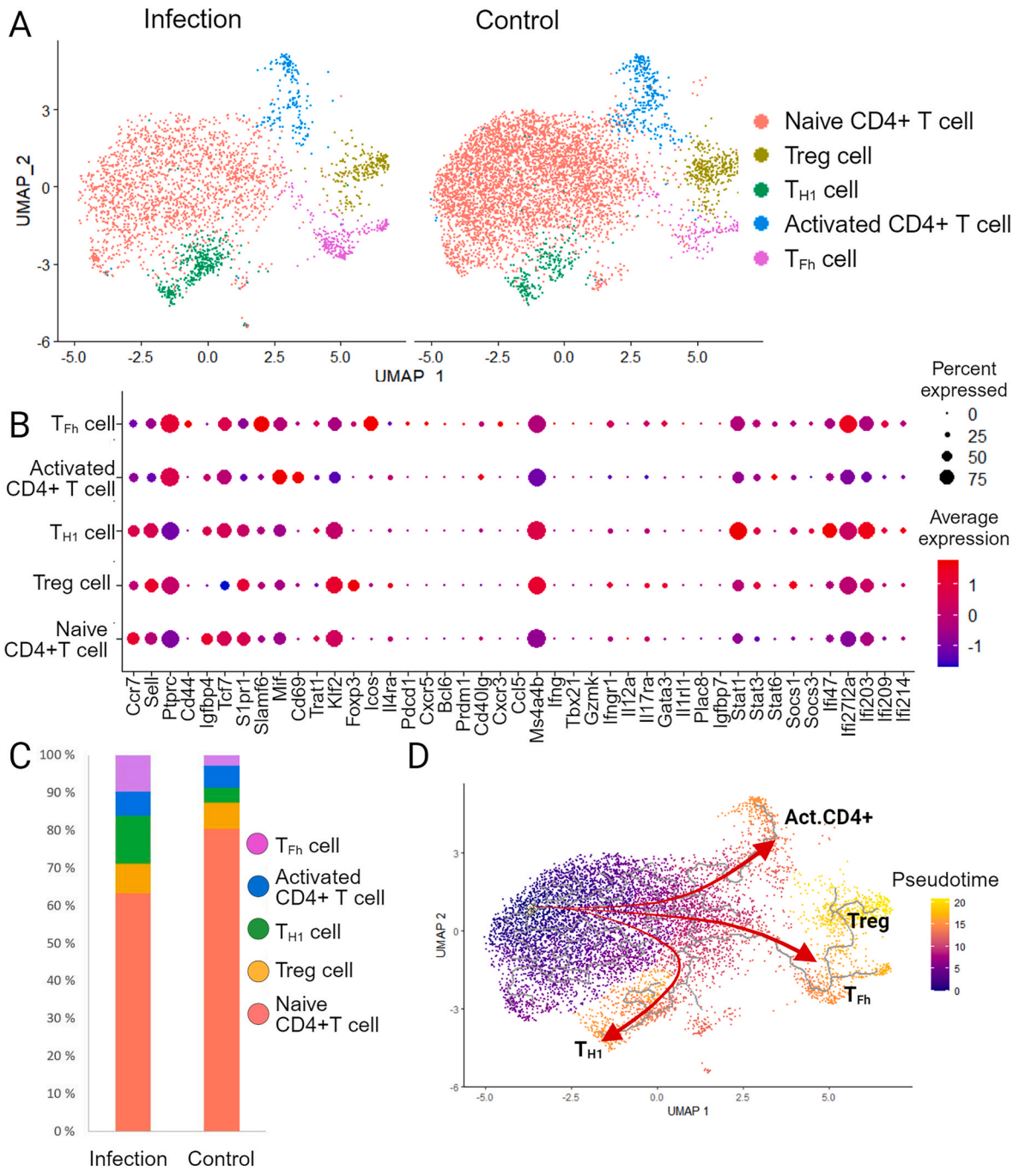

Fig. 5. $CD4^+$ T cell subset classification

(A) UMAP projection of identified $CD4^+$ T cell clusters of infection and control groups. Cell clusters are shown in different colours. (B) Dot plot representing the gene expression profile of selected marker genes of $CD4^+$ cell lineages. (C) The comparison of relative frequencies of cells in $CD4^+$ T cell lineages in the infection and the control groups. (D) Pseudotime analysis of $CD4^+$ T cell subset. Red arrows are pointing out possible differentiation pathways of activated $CD4^+$ T, Treg, T_{Fh}, and T_{H1} cells from top to bottom, respectively.

in the control group (p-value <0.00001). Treg cells formed relatively the same proportion of cells between the infection and the control group (p-value = 0.0829). We were unable to see whether *B. burgdorferi* infection induces more T_{Fh} cell or T_{H1} cell differentiation, likely due to the early stage of the infection. Trajectory and pseudotime analysis of the $CD4^+$ T cell subset suggests potential differentiation pathways toward activated $CD4^+$ T, Treg, T_{Fh}, and T_{H1} cells (Fig. 5 D). Furthermore, T_{Fh} and Treg cells are potentially differentiated earlier compared to T_{H1} and activated $CD4^+$ cells, which is indicated by their differentiation status in pseudotime.

Signal transducer and activator of transcription 1 (*Stat1*; p-adj. = 2.8534e-140, Log2FC = 0.8508) and several interferon-induced genes e. g. interferon gamma inducible protein 47 (*Ifi47*; p-adj. = 2.4263e-76 Log2FC = 0.6186) and interferon gamma induced GTPase (*Igtp*; p-adj. = 1.3792e-121, Log2FC = 0.8285), displayed upregulation in the infection group (Fig. 6A). Since *Stat1* is essential for T_{H1} differentiation, its expression may reflect infection-induced T_{H1} cell differentiation. Interestingly, despite the T_{H1} cell differentiation, there was no evidence of *Ifng* (interferon-gamma encoding gene) expression in the infection group (Fig. 5B, Supplementary Fig. 4C). The analysis of significantly changed

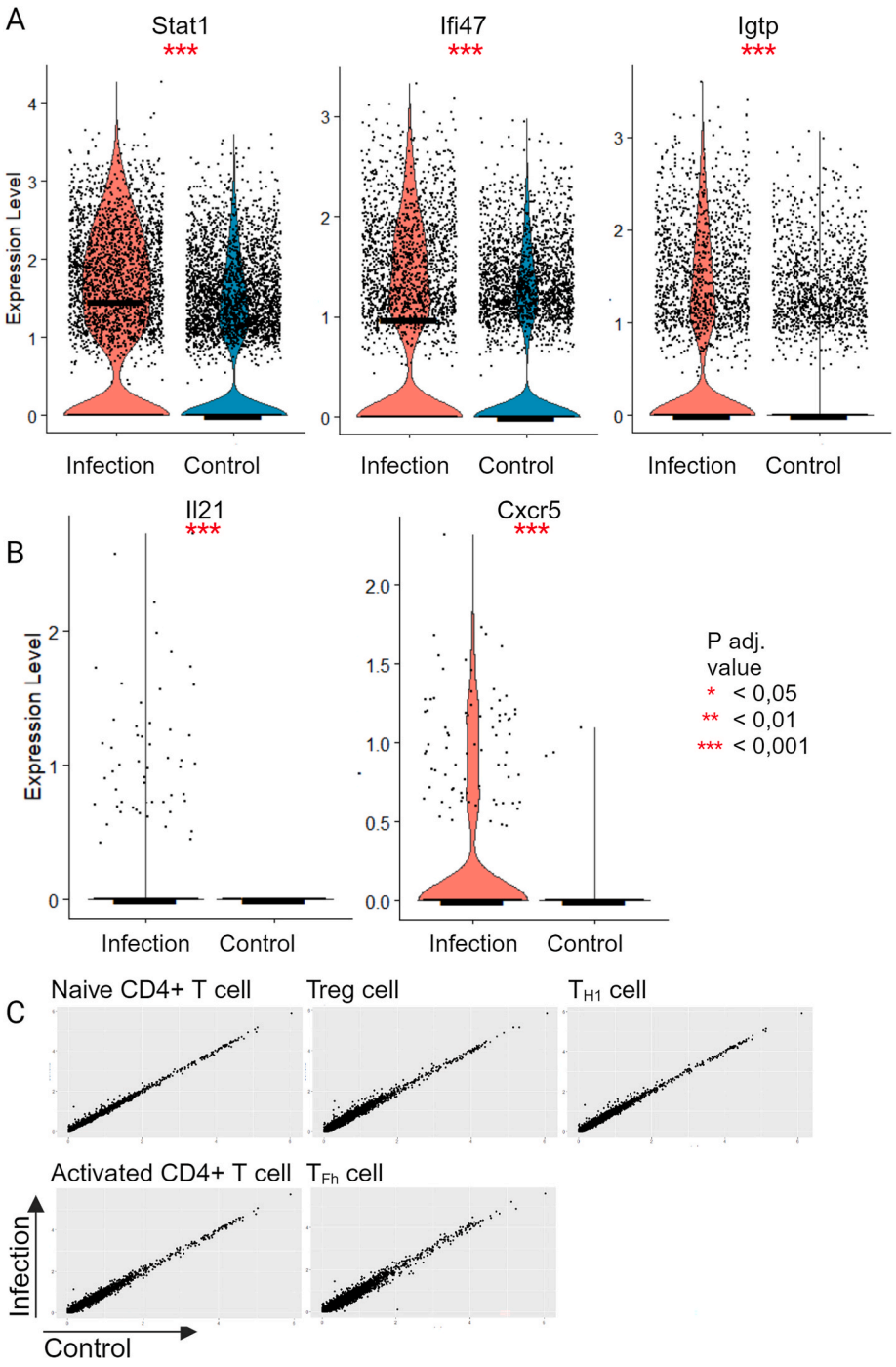

Fig. 6. Differentially expressed genes in $CD4^+$ T cells between the infection and the control group
(A) Violin plot representation with medians of *Stat1* and some interferon-induced genes (*Ifi47, Igtp*), which were significantly upregulated in the infection group. Significances are pointed out with red asterisks. (B) Violin plot representation with expression of *Il21* and *Cxcr5* in T_{Fh} cell subset of the infection group compared to the control group. (C) Scatter plots representing the average gene expression of $CD4^+$ T cell clusters in the infection and the control groups, highlighting the similarity of the datasets despite the infection. X-axis represents the average gene expression of the control group and the Y-axis represents the average gene expression of the infection group. * = adjusted P value < 0.05; ** = adjusted P value < 0.01; *** = adjusted P value < 0.001.

gene expression of T_{Fh} cells between the control and the infection groups, suggested that some of the T_{Fh} cells were prepared for germinal centre responses in the infection group (Fig. 6B). *Il21*, the gene encoding a cytokine that is critical for germinal centre formation (p-adj. = 3.4748e-04, Log2FC = 0.5447), and *Cxcr5*, the gene encoding chemokine receptor 5 that localizes T_{Fh} cells to developing germinal centres (p-adj. = 2.3174e-07, Log2FC = 0.5496), were upregulated by T_{Fh} cells in the infection group. While the differences were statistically significant, only a small pool of T_{Fh} cells in the infection group showed expression of *Il21* and *Cxcr5*.

In conclusion, $CD4^+$ T cells reflected broadly similar transcriptomic profiles in the infection and control groups (Fig. 6C). Only a few cells displayed detectable expression of cell proliferation marker *Mki67*, indicating that the $CD4^+$ T cell population was not significantly activated (Supplementary Fig. 4D). However, the increases in T_{Fh} and T_{H1} cells suggest that there is some activation due to *B. burgdorferi* infection.

4. Discussion

This study describes scRNA-seq profiling of lymph node lymphocytes in *B. burgdorferi* infection in mice. We focused on the early immune response, which primarily involves extrafollicular B cell responses, and found infection-induced upregulation of suppressor of cytokine signalling genes *Socs1* and *Socs3* in B cells. Our results suggest a model where *Socs3*-mediated regulation restricts T – B cell interaction in early B. *burgdorferi* infection.

In support of our hypothesis of a limited B and T cell interaction, earlier studies of mice infected with *B. burgdorferi* have demonstrated a failure in the development of protective immunity after vaccination with influenza antigens, underscoring the inhibitory effect of *B. burgdorferi* on the development of long-term humoral immunity [6]. The exact molecular mechanisms behind the phenomenon have remained obscure, even though it has been studied broadly for example with flow cytometry and histology [5,9,19,24].

In recent years, the heterogeneity of gene expression within cell populations has become increasingly evident [27,28]. ScRNA-seq approach has been successfully applied to analyse for example the heterogeneity of tumours and cellular developmental pathways with high resolution. Studies of single-cell transcriptomic profiles in infection immunity have remained relatively limited but have underscored, e.g., a key role for B cells in response to *B. burgdorferi* in the erythema migrans lesions, and revealed transcriptional changes following *B. burgdorferi* infection in murine ankle joints [29,30].

Using single-cell RNA sequencing, we found that B cells were highly abundant in mouse lymph nodes after infection, while T cells represented a smaller proportion. A rapid enlargement of the regional inguinal lymph nodes has previously been observed, for example starting at day four in *B. burgdorferi*-infected C57BL/6 mice, where the increased lymph node cellularity was shown to be due to a massive expansion of B cells [9,31]. The accumulation of B cells may disturb germinal centre formation, and the resulting lack of functional germinal centres or failure to maintain them leads to inability to generate long-lived plasma cells and efficient B cell memory [6,11,27]. Indeed, Hastey et al. found a clear demarcation of T and B cell zones only until day four of the *B. burgdorferi* infection, and the increase in B cell frequency was accompanied by a corresponding decrease in $CD4^+$ T cell frequency [19]. In line with our results, $CD4^+$ T cells have been shown to differentiate into T follicular helper phenotypic cells following *B. burgdorferi* infection, suggesting that there is not a total defect in T cell responses, but rather T-dependent responses are suppressed, which could contribute to the mainly extrafollicular immune response [6,11].

We sought insight into the reasons behind the mainly extrafollicular *B. burgdorferi*-specific B cell responses by focusing on the early time point of the infection [24]. In our model, the activation and accumulation of B cells in lymph nodes of *B. burgdorferi* infected mice are consistent with the results of previous studies [9,32,33]. Our results indicate that within just four days, *B. burgdorferi* infection triggers a notable B cell proliferation, immunoglobulin class switching to IgG3 and IgG2b isotypes, and induces plasma cell differentiation, all hallmarks of extrafollicular immune response [10]. The extrafollicular response was further supported by immunohistochemistry. The expression of TACI (*Tnfrsf13b*) further suggests that immunoglobulin class switching is induced during the extrafollicular immune response and high expression of *Cxcr4* in PB draws them to extrafollicular regions, particularly to medullary cords [34–37]. Interestingly, the most upregulated genes of B cells of the infection group have similarity to the reported gene expression patterns in mice during *Salmonella* infection, which is also known to trigger an extrafollicular response [25]. Importantly, there was no evidence of high *Bcl6* expression in any of the B cell clusters, demonstrating the lack of germinal centre response. These findings are in line with previously described predominantly extrafollicular responses to *B. burgdorferi* [4,9].

We found that both T_{H1} and T_{Fh} cell populations were more abundant in the infection group compared to the control group and the upregulation of *Il21* and *Cxcr5* in T_{Fh} cells suggests that some of the cells were instructed for germinal centre reactions. Strong T_{H1} differentiation with the lack of T_{Fh} cells would have the potential to explain why the immune response during *B. burgdorferi* infection fails to maintain T-dependent germinal centre responses. However, the early stage of the infection does not allow for the determination of whether *B. burgdorferi* infection primarily drives T_{H1} or T_{Fh} cell differentiation. Previous findings suggest that *B. burgdorferi* infection is T_{H1} dominant [38]. Four days after infection, we could not see any induction of *Ifng* (encoding interferon-gamma) expression, despite the seemingly initiated differentiation into T_{H1} cells. Our data suggest that interferon-gamma is rather secreted by other cells than the T_{H1} cell population. However, neither natural killer cells, macrophages nor dendritic cells of our dataset showed expression of *Ifng* (data not shown). Hammond et al. have recently reported similar results at a later time point [11]. Their data suggest that *B. burgdorferi* infection does not induce interferon-gamma producing $CD4^+$ cells in lymph nodes.

Earlier, *B. burgdorferi* infection has been hypothesized to induce restricted T cell responses, possibly through increased expression of *Socs3* in dendritic cells, macrophages, and monocytes leading to reduced antigen presentation to T cells [39,40]. In macrophages, *B. burgdorferi* spirochetes or lipidated outer surface protein A (*L-OspA*) increases *Socs1* and *Socs3* mRNA and protein expression [40]. Such an effect has not been described in B cells until now. Our data indicate that a Socs-mediated downregulation of the antigen presentation pathway may also be active in B cells.

In the context of many bacterial infections, *Ciita* expression is induced in B cells. CIITA is a major transcription factor promoting the expression of the MHC II molecules during antigen presentation to T helper cells [41]. *Ciita* transcription, in turn, is directly promoted by STAT1 [42]. Contrary to our expectations, we did not observe infection-driven upregulation of MHC II-related genes. Instead, many of the genes, including *Ciita*, were consistently downregulated, although not all the differences reached statistical significance. One plausible interpretation arising from this analysis is that the observed negative regulation of receptor signalling pathways via STAT/JAK-STAT in *B. burgdorferi* infection results from *Socs1* and *Socs3* upregulation. These inhibitors of JAK-STAT signalling could cause the downregulation of genes of MHC II antigen presentation, and of other genes regulating B-T cell interactions and thus preventing B cells from receiving adequate T cell help. These findings may provide a partial explanation for why *B. burgdorferi* directs the immune response toward the extrafollicular B cell pathway. Our results suggest that the impaired germinal centre responses in *B. burgdorferi* infection are driven by a strong extrafollicular response and/or restricted B - T cell communication.

B. burgdorferi has a multitude of strategies and mechanisms to evade both natural and adaptive immune responses [43]. The sequential expression of a vast array of outer surface lipoproteins on the spirochete allows the bacteria to establish a persistent infection. For example, BBK32 and CRASP proteins interfere with the activation of the complement system. The vlsE gene encodes the outer surface lipoprotein VlsE [43–47], which is continuously modified as the gene undergoes segmental conversion events with the 15 adjacently located silent gene cassettes, and creates continuously new variants of the antigen allowing an enormous potential for antigenic variation. In nature, during the early events of a tick-borne infection, tick saliva proteins protect the bacteria from the immune response in many ways. For instance, Salp15, one of the proteins, binds to OspC lipoprotein on the spirochete surface preventing the formation of the membrane attack complex of the complement system. OspC expression, and the simultaneous OspA downregulation, is on the other hand turned on during the tick blood feeding on a host animal [48]. Tick saliva also inhibits lymphocyte proliferation and antibody production by B cells [49]. Thus, the use of in vitro-grown *B. burgdorferi*, which express mainly OspA, and the syringe inoculation of bacteria, constitute a weakness in the present study, and the observed

immune response in the lymph nodes might be different from the response during natural *B. burgdorferi* infection [48,50]. Nonetheless, our results are parallel to typical immune response patterns described in tick-borne *B. burgdorferi* infections [9]. In addition, our results allow the identification of a new potential suppressive mechanism of T lymphocyte activation in *B. burgdorferi* infection.

Taken together, our results highlight the role of B cells in the immune response to *B. burgdorferi* infection. The gene expression patterns observed at the early time-point of the infection suggest a predominantly extrafollicular immune response characterized by the secretion of IgG2b and IgG3 by short-lived plasma cells. In the future, analysis of T and B cell interactions during *B. burgdorferi* infection at later time points and with control infections would provide a more comprehensive view of the balance between extrafollicular and germinal centre responses.

Ethics approval

All animal experiments were approved by the Ethical Committee for Animal Experimentation in Finland. Experiments were performed according to the Finnish Act on Animal Experimentation (497/2013) in compliance with the 3R-principle with the appropriate animal license (ESAVI/6265/04.July 10, 2017).

CRediT authorship contribution statement

Varpu Rinne: Investigation, Methodology, Visualization, Writing – original draft, Writing – review & editing, Data curation, Formal analysis. **Kirsi Gröndahl-Yli-Hannuksela:** Investigation, Methodology, Writing – original draft, Writing – review & editing, Conceptualization, Data curation, Formal analysis. **Ruth Fair-Mäkelä:** Investigation, Methodology, Visualization, Formal analysis, Writing – review & editing. **Marko Salmi:** Writing – review & editing, Conceptualization, Investigation. **Pia Rantakari:** Investigation, Methodology, Writing – review & editing. **Tapio Lönnberg:** Investigation, Methodology, Writing – review & editing. **Jukka Alinikula:** Conceptualization, Supervision, Writing – review & editing, Investigation. **Annukka Pietikäinen:** Conceptualization, Methodology, Supervision, Writing – review & editing, Funding acquisition, Investigation. **Jukka Hytönen:** Conceptualization, Funding acquisition, Supervision, Writing – review & editing, Investigation, Project administration, Resources.

Acknowledgements

This work was supported by the Special Governmental Fund for University Hospitals, and the Sakari Alhopuro foundation. We thank Finnish Functional Genomics Centre supported by University of Turku, Åbo Akademi University, and Biocenter Finland, and Single Cell Omics Facility of Turku Bioscience. Figures of this article were created with Biorender.com.

Appendix A. Supplementary data

Supplementary data to this article can be found online at https://doi.org/10.1016/j.micinf.2024.105424.

References

[1] Stanek G, Wormser GP, Gray J, Strle F. Lyme borreliosis. Lancet 2012;379:461–73. https://doi.org/10.1016/S0140-6736(11)60103-7.
[2] Mead PS. Epidemiology of Lyme disease. Infect Dis Clin North Am 2015;29:187–210. https://doi.org/10.1016/j.idc.2015.02.010.
[3] Tracy KE, Baumgarth N. Borrelia burgdorferi manipulates innate and adaptive immunity to establish persistence in rodent reservoir hosts. Front Immunol 2017;8. https://doi.org/10.3389/fimmu.2017.00116.
[4] Bockenstedt LK, Wooten RM, Baumgarth N. Immune response to *Borrelia* : lessons from Lyme disease spirochetes. Curr Issues Mol Biol 2022:145–90. https://doi.org/10.21775/cimb.042.145.
[5] Elsner RA, Hastey CJ, Baumgarth N. CD4 $^{+}$ T cells promote antibody production but not sustained affinity maturation during Borrelia burgdorferi infection. Infect Immun 2015;83:48–56. https://doi.org/10.1128/IAI.02471-14.
[6] Elsner RA, Hastey CJ, Olsen KJ, Baumgarth N. Suppression of long-lived humoral immunity following Borrelia burgdorferi infection. PLoS Pathog 2015;11:e1004976. https://doi.org/10.1371/journal.ppat.1004976.
[7] Paus D, Phan TG, Chan TD, Gardam S, Basten A, Brink R. Antigen recognition strength regulates the choice between extrafollicular plasma cell and germinal center B cell differentiation. J Exp Med 2006;203:1081–91. https://doi.org/10.1084/jem.20060087.
[8] Yegutkin GG, Hytönen J, Samburski SS, Yrjänäinen H, Jalkanen S, Viljanen MK. Disordered lymphoid purine metabolism contributes to the pathogenesis of persistent *Borrelia garinii* infection in mice. J Immunol 2010;184:5112–20. https://doi.org/10.4049/jimmunol.0902760.
[9] Tunev SS, Hastey CJ, Hodzic E, Feng S, Barthold SW, Baumgarth N. Lymphoadenopathy during Lyme borreliosis is caused by spirochete migration-induced specific B cell activation. PLoS Pathog 2011;7:e1002066. https://doi.org/10.1371/journal.ppat.1002066.
[10] Elsner RA, Shlomchik MJ. Germinal center and extrafollicular B cell responses in vaccination, immunity, and autoimmunity. Immunity 2020;53:1136–50. https://doi.org/10.1016/j.immuni.2020.11.006.
[11] Hammond EM, Olsen KJ, Ram S, Tran GVV, Hall LS, Bradley JE, et al. Antigen-specific CD4 T cell and B cell responses to *Borrelia burgdorferi*. J Immunol 2023. https://doi.org/10.4049/jimmunol.2200890.
[12] Salo J, Jaatinen A, Söderström M, Viljanen MK, Hytönen J. Decorin binding proteins of Borrelia burgdorferi promote arthritis development and joint specific post-treatment DNA persistence in mice. PLoS One 2015;10:e0121512. https://doi.org/10.1371/journal.pone.0121512.
[13] Cuellar J, Pietikäinen A, Glader O, Liljenbäck H, Söderström M, Hurme S, et al. Borrelia burgdorferi infection in biglycan knockout mice. J Infect Dis 2019;220:116–26. https://doi.org/10.1093/infdis/jiz050.
[14] Hao Y, Hao S, Andersen-Nissen E, Mauck WM, Zheng S, Butler A, et al. Integrated analysis of multimodal single-cell data. Cell 2021;184:3573–3587.e29. https://doi.org/10.1016/J.CELL.2021.04.048.
[15] Zhou Y, Zhou B, Pache L, Chang M, Khodabakhshi AH, Tanaseichuk O, et al. Metascape provides a biologist-oriented resource for the analysis of systems-level datasets. Nat Commun 2019;10:1523. https://doi.org/10.1038/s41467-019-09234-6.
[16] Cao J, Spielmann M, Qiu X, Huang X, Ibrahim DM, Hill AJ, et al. The single-cell transcriptional landscape of mammalian organogenesis. Nature 2019;566:496–502. https://doi.org/10.1038/s41586-019-0969-x.
[17] Edgar R. Gene Expression Omnibus: NCBI gene expression and hybridization array data repository. Nucleic Acids Res 2002;30:207–10. https://doi.org/10.1093/nar/30.1.207.
[18] Wang H, Jain S, Li P, Lin J-X, Oh J, Qi C, et al. Transcription factors IRF8 and PU.1 are required for follicular B cell development and BCL6-driven germinal center responses. Proc Natl Acad Sci USA 2019;116:9511–20. https://doi.org/10.1073/pnas.1901258116.
[19] Hastey CJ, Ochoa J, Olsen KJ, Barthold SW, Baumgarth N. MyD88- and TRIF-independent induction of type I interferon drives naive B cell accumulation but not loss of lymph node architecture in Lyme disease. Infect Immun 2014;82:1548–58. https://doi.org/10.1128/IAI.00969-13.
[20] Hargreaves DC, Hyman PL, Lu TT, Ngo VN, Bidgol A, Suzuki G, et al. A coordinated change in chemokine responsiveness guides plasma cell movements. J Exp Med 2001;194:45–56. https://doi.org/10.1084/jem.194.1.45.
[21] Johnson RM, Kerr MS, Slaven JE. *Plac8* -dependent and inducible NO synthase-dependent mechanisms clear *Chlamydia muridarum* infections from the genital tract. J Immunol 2012;188:1896–904. https://doi.org/10.4049/jimmunol.1102764.
[22] Ledford JG, Kovarova M, Koller BH. Impaired host defense in mice lacking ONZIN. J Immunol 2007;178:5132–43. https://doi.org/10.4049/jimmunol.178.8.5132.
[23] Kincaid EZ, Che JW, York I, Escobar H, Reyes-Vargas E, Delgado JC, et al. Mice completely lacking immunoproteasomes show major changes in antigen presentation. Nat Immunol 2012;13:129–35. https://doi.org/10.1038/ni.2203.
[24] Hastey CJ, Elsner RA, Barthold SW, Baumgarth N. Delays and diversions mark the development of B cell responses to *Borrelia burgdorferi* infection. J Immunol 2012;188:5612–22. https://doi.org/10.4049/jimmunol.1103735.
[25] Cunningham AF, Gaspal F, Serre K, Mohr E, Henderson IR, Scott-Tucker A, et al. *Salmonella* induces a switched antibody response without germinal centers that impedes the extracellular spread of infection. J Immunol 2007;178:6200–7. https://doi.org/10.4049/jimmunol.178.10.6200.
[26] Xin P, Xu X, Deng C, Liu S, Wang Y, Zhou X, et al. The role of JAK/STAT signaling pathway and its inhibitors in diseases. Int Immunopharmacol 2020;80:106210. https://doi.org/10.1016/j.intimp.2020.106210.
[27] Hwang B, Lee JH, Bang D. Single-cell RNA sequencing technologies and bioinformatics pipelines. Exp Mol Med 2018;50:1–14. https://doi.org/10.1038/s12276-018-0071-8.
[28] Chen G, Ning B, Shi T. Single-cell RNA-seq technologies and related computational data analysis. Front Genet 2019;10. https://doi.org/10.3389/fgene.2019.00317.
[29] Jiang R, Meng H, Raddassi K, Fleming I, Hoehn KB, Dardick KR, et al. Single-cell immunophenotyping of the skin lesion erythema migrans identifies IgM memory B cells. JCI Insight 2021;6:e148035. https://doi.org/10.1172/jci.insight.148035.
[30] Helble JD, Walsh MJ, McCarthy JE, Smith NP, Tirard AJ, Arnold BY, et al. Single-cell RNA sequencing of murine ankle joints over time reveals distinct transcriptional changes following Borrelia burgdorferi infection. iScience 2023;26:108217. https://doi.org/10.1016/j.isci.2023.108217.

[31] Sigal LH, Steere AC, Dwyer JM. In vivo and in vitro evidence of B cell hyperactivity during Lyme disease. J Rheumatol 1988;15:648–54.
[32] Honarvar N, Schaible UE, Galanos C, Wallich R, Simon MM. A 14,000 MW lipoprotein and a glycolipid-like structure of Borrelia burgdorferi induce proliferation and immunoglobulin production in mouse B cells at high frequencies. Immunology 1994;82:389–96.
[33] Yang L, Ma Y, Schoenfeld R, Griffiths M, Eichwald E, Araneo B, et al. Evidence for B-lymphocyte mitogen activity in Borrelia burgdorferi-infected mice. Infect Immun 1992;60:3033–41. https://doi.org/10.1128/iai.60.8.3033-3041.1992.
[34] He B, Santamaria R, Xu W, Cols M, Chen K, Puga I, et al. The transmembrane activator TACI triggers immunoglobulin class switching by activating B cells through the adaptor MyD88. Nat Immunol 2010;11:836–45. https://doi.org/10.1038/ni.1914.
[35] MacLennan ICM, Toellner K, Cunningham AF, Serre K, Sze DM-Y, Zúñiga E, et al. Extrafollicular antibody responses. Immunol Rev 2003;194:8–18. https://doi.org/10.1034/j.1600-065X.2003.00058.x.
[36] Wehrli N, Legler DF, Finke D, Toellner K-M, Loetscher P, Baggiolini M, et al. Changing responsiveness to chemokines allows medullary plasmablasts to leave lymph nodes. Eur J Immunol 2001;31:609–16. https://doi.org/10.1002/1521-4141(200102)31:2<609::AID-IMMU609>3.0.CO. 2-616.
[37] Brighenti A, Andrulis M, Geissinger E, Roth S, Müller-Hermelink HK, Rüdiger T. Extrafollicular proliferation of B cells in the absence of follicular hyperplasia: a distinct reaction pattern in lymph nodes correlated with primary or recall type responses. Histopathology 2005;47:90–100. https://doi.org/10.1111/j.1365-2559.2005.02173.x.
[38] Ganapamo F, Dennis VA, Philipp MT. Early induction of gamma interferon and interleukin-10 production in draining lymph nodes from mice infected with *Borrelia burgdorferi*. Infect Immun 2000;68:7162–5. https://doi.org/10.1128/IAI.68.12.7162-7165.2000.
[39] Brouwer MAE, Jones-Warner W, Rahman S, Kerstholt M, Ferreira AV, Oosting M, et al. B. burgdorferi sensu lato-induced inhibition of antigen presentation is mediated by RIP1 signaling resulting in impaired functional T cell responses towards Candida albicans. Ticks Tick Borne Dis 2021;12:101611. https://doi.org/10.1016/j.ttbdis.2020.101611.
[40] Dennis VA, Jefferson A, Singh SR, Ganapamo F, Philipp MT. Interleukin-10 anti-inflammatory response to Borrelia burgdorferi, the agent of Lyme disease: a possible role for suppressors of cytokine signaling 1 and 3. Infect Immun 2006;74:5780–9. https://doi.org/10.1128/IAI.00678-06.
[41] Piskurich JF, Gilbert CA, Ashley BD, Zhao M, Chen H, Wu J, et al. Expression of the MHC class II transactivator (CIITA) type IV promoter in B lymphocytes and regulation by IFN-γ. Mol Immunol 2006;43:519–28. https://doi.org/10.1016/j.molimm.2005.05.005.
[42] Muhlethaler-Mottet A, Di Berardino W, Otten LA, Mach B. Activation of the MHC class II transactivator CIITA by interferon-γ requires cooperative interaction between Stat1 and USF-1. Immunity 1998;8:157–66. https://doi.org/10.1016/S1074-7613(00)80468-9.
[43] Anderson C, Brissette CA. The brilliance of Borrelia: mechanisms of host immune evasion by Lyme disease-causing spirochetes. Pathogens 2021;10:281. https://doi.org/10.3390/pathogens10030281.
[44] Lawrenz MB, Hardham JM, Owens RT, Nowakowski J, Steere AC, Wormser GP, et al. Human antibody responses to VlsE antigenic variation protein of Borrelia burgdorferi. J Clin Microbiol 1999;37:3997–4004. https://doi.org/10.1128/JCM.37.12.3997-4004.1999.
[45] Bankhead T, Chaconas G. The role of VlsE antigenic variation in the Lyme disease spirochete: persistence through a mechanism that differs from other pathogens. Mol Microbiol 2007;65:1547–58. https://doi.org/10.1111/j.1365-2958.2007.05895.x.
[46] Rogovskyy AS, Casselli T, Tourand Y, Jones CR, Owen JP, Mason KL, et al. Evaluation of the importance of VlsE antigenic variation for the enzootic cycle of Borrelia burgdorferi. PLoS One 2015;10:e0124268. https://doi.org/10.1371/journal.pone.0124268.
[47] Winslow C, Coburn J. Recent discoveries and advancements in research on the Lyme disease spirochete Borrelia burgdorferi. F1000Res 2019;8. https://doi.org/10.12688/f1000research.18379.1.
[48] de Silva AM, Telford SR, Brunet LR, Barthold SW, Fikrig E. Borrelia burgdorferi OspA is an arthropod-specific transmission-blocking Lyme disease vaccine. J Exp Med 1996;183:271–5. https://doi.org/10.1084/jem.183.1.271.
[49] Kotál J, Langhansová H, Lieskovská J, Andersen JF, Francischetti IMB, Chavakis T, et al. Modulation of host immunity by tick saliva. J Proteomics 2015;128:58–68. https://doi.org/10.1016/j.jprot.2015.07.005.
[50] Xu Q, McShan K, Liang FT. Two regulatory elements required for enhancing ospA expression in Borrelia burgdorferi grown in vitro but repressing its expression during mammalian infection. Microbiology (Read) 2010;156:2194–204. https://doi.org/10.1099/mic.0.036608-0.